Sensors & Actuators: B. Chemical 376 (2023) 132980

Contents lists available at ScienceDirect

Sensors and Actuators: B. Chemical

journal homepage: www.elsevier.com/locate/snb

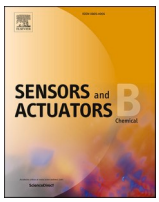

Cellular membrane imaging of the dynamic binding-dissociation of rhodamine-benzenesulfonamide bioconjugate with carbonic anhydrase IX for inhibitor screening

Wei Zhou [a,b], Qinglong Qiao [b,*], Yi Tao [b], Wenchao Jiang [b], Xiangning Fang [b], Jin Li [b], Ning Xu [b], Zhaochao Xu [a,b,**]

[a] Zhang Dayu School of Chemistry, Dalian University of Technology, Dalian 116012, China
[b] CAS Key Laboratory of Separation Science for Analytical Chemistry, Dalian Institute of Chemical Physics, Chinese Academy of Sciences, Dalian 116023, China

ARTICLE INFO

Key words:
Cellular membrane imaging
Carbonic anhydrase IX
Dynamic binding-dissociation
Benzenesulfonamide
Inhibitor screening

ABSTRACT

Fluorescent displacement assay has been used as an effective method to screen target protein inhibitors, but there is a lack of reports on the detection of small molecule inhibitor activity by tracking the binding and dissociation of fluorescent substrates to target proteins in living cells. In this paper, we synthesized a cell membrane-impermeable benzenesulfonamide-conjugated rhodamine 6G derivative, **CA532**, which dynamically binds to cells expressing carbonic anhydrase IX (CAIX) for fluorescence imaging of cell membranes, while small molecule inhibitors competitively displace **CA532** from CAIX, resulting in a decrease in the fluorescence intensity on the cell membrane. The activity of different inhibitors cause concentration-dependent dynamic binding and dissociation of protein-substrate complexes, and the associated diverse replacement processes can be fully revealed by fluorescence imaging of cell membranes, which also enables **CA532** to screen CAIX inhibitors in situ in living cells.

1. Introduction

Cell membrane proteins provide numerous vital biological functions in cell physiology, such as catalysis of enzymes, transport, signal transmission, cell recognition, intercellular joining and attachment [1–3]. A large number of human disorders were linked to aberrant membrane proteins; in fact, over sixty percent of FDA-approved small molecule therapies targeted cell membrane proteins [4]. Therefore, it is essential to develop screening and detection methods for membrane protein inhibitors. Molecular computing and high-throughput screening of molecular libraries were the traditional methods for drug discovery [5]. Detection of protein binding ability, for instance, frequently necessitates the identification of pure proteins in test tubes employing fluorescence [6–8], NMR [9], mass spectrometry [10], and other techniques [11,12]. However, membrane proteins, unlike cytoplasmic proteins, are located in the hydrophobic lipid bilayer of the cell membrane, which makes in vitro biochemical activities such as protein expression and purification extremely difficult [13,14]. Additionally, when membrane proteins are removed from their natural environment, they may lose vital biological properties. Therefore, it is highly desirable to develop inhibitor-finding strategies that are compatible with normal physiological circumstances for membrane proteins.

Carbonic anhydrase IX (CAIX) is a transmembrane zinc metalloenzyme that catalyzes the reversible hydration of carbon dioxide into bicarbonate ions and protons [15]. CAIX belongs to the α class of the family of carbonic anhydrases (CAs) expressed in higher vertebrate. Its crucial role in intracellular pH maintenance represents the mechanism by which cancer cells adapt to the emergency conditions of the extracellular environment. In addition, CAIX protein activity enhances cancer cell migration and is associated with an increase in the aggressive/invasive aspect of malignancies. Since it is expressed in a range of tumor types, CAIX protein is recognized as a marker of tumor hypoxia. Its expression is tightly connected with the clinical outcome prognosis for a variety of tumor types [16]. All of the aforementioned evidence demonstrates CAIX's outstanding potential as a pharmaceutical therapeutic target [17,18]. Regardless of the fact that indicator displacement

* Corresponding author.
** Corresponding author at: Zhang Dayu School of Chemistry, Dalian University of Technology, Dalian 116012, China.
E-mail addresses: qqlqiao@dicp.ac.cn (Q. Qiao), zcxu@dicp.ac.cn (Z. Xu).

https://doi.org/10.1016/j.snb.2022.132980
Received 11 October 2022; Received in revised form 7 November 2022; Accepted 9 November 2022
Available online 12 November 2022

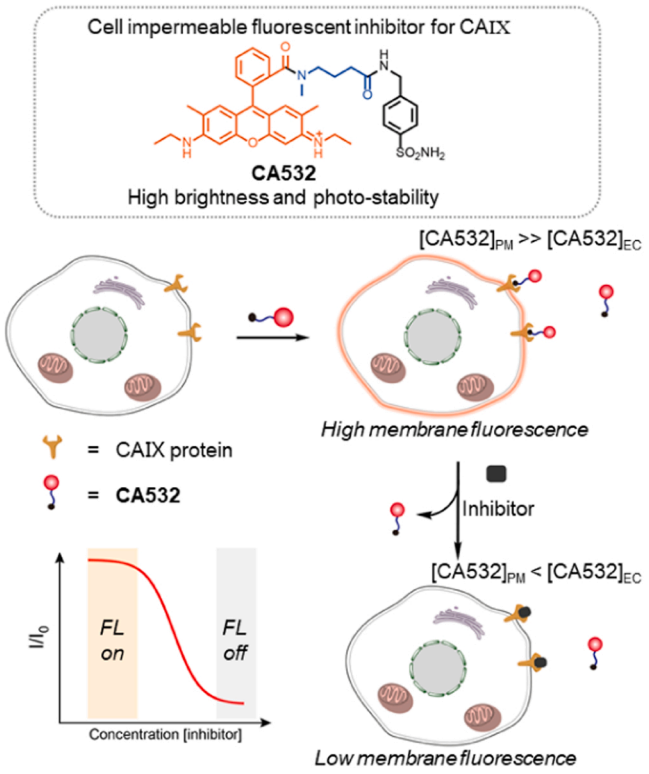

Fig. 1. Schematic illustration of wash-free imaging of plasma membrane CAIX protein and fluorescence competition assay by the probe **CA532**. $[\mathbf{CA532}]_{PM}$ represents the dye concentration on the cell membrane; $[\mathbf{CA532}]_{EC}$ represents the dye concentration outside the cell membrane.

assays (IDAs) have enabled the detection of numerous target inhibitors [6,19–24], there still have no simple and uncomplicated method for identifying membrane protein CAIX inhibitors in situ.

In contrast to competitive detection of protein inhibitors in test tubes or intracellular environment, inhibitor screening for cell membrane proteins requires the probe to be environmentally insensitive and incapable of penetrating the cell membrane for an extended period of time, thereby reducing intracellular signal interference and enhancing detection accuracy [25]. In this paper, we conjugated the environmentally insensitive dye rhodamine 6G with the CA protein targeted small molecular benzenesulfonamide through a modified methamphetamine linker to obtain the probe **CA532** as shown in Fig. 1. The existence of tertiary amide makes **CA532** stable in the zwitterionic form that is not suitable for membrane permeation and cannot form the spirolactam form which is easily permeable to membranes [26,27]. The very short linking group and multiple amide bonds make **CA532** not aggregated and can be stably dispersed outside the living cells, which makes the very low concentration of **CA532** outside the cell membrane will not cause signal interference to cell membrane imaging. When **CA532** binds to CAIX and aggregates on the cell membrane, the local high concentration of probe produces high fluorescence brightness, which makes the cell membrane imaging without washing to remove excess dye molecules outside the cell membrane and has an excellent signal-to-noise ratio. When a competitive inhibitor is added, **CA532** is displaced into the cell culture medium and fluorescence is diminished. Using differences in real-time fluorescence intensity on the cell membranes, the activities of CAIX inhibitors would be imaged in-situ.

2. Experimental section

2.1. Synthesis

2.1.1. Synthesis of Rho6G-MABA

Rho6G-COOH (200 mg, 0.48 mmol), EDCI (110 mg, 0.57 mmol) and N-Hydroxysuccinimide (66 mg, 0.57 mmol) were dissolved in 15 mL dichloromethane and the solution was stirred for 12 h. The solvent was removed under reduced pressure to obtain purple red solid without further purification. The residue was dissolved in 15 mL acetonitrile (ACN) and 60 mg K_2CO_3, and 4-(methylamino)butanoic acid (154 mg, 1.38 mmol) were next added to the solution. After stirred for 12 h at room temperature, the solvent was removed under reduced pressure and the residue was further purified by silica gel chromatography (MeOH /DCM = 10:1; V/V) to afforded **Rho6G-MABA** as a purple red solid 74 mg, yield 30 % . ^{1}H NMR (400 MHz, DMSO-d_6) δ 7.88 (s, 2 H), 7.75–7.61 (m, J = 8.7, 5.1 Hz, 3 H), 7.54–7.44 (m, 1 H), 6.94 (s, 2 H), 6.86 (s, 2 H), 3.48 (q, J = 6.9 Hz, 4 H), 3.10 (t, 2 H), 2.90 (s, 3 H), 2.15 (s, 6 H), 1.68 (t, J = 7.3 Hz, 2 H), 1.27–1.22 (m, J = 7.1 Hz, 8 H). ^{13}C NMR (100 MHz, DMSO-d_6) δ 174.14, 167.92, 157.07, 156.23, 136.89, 132.15, 131.25, 130.60, 130.03, 129.86, 129.62, 127.68, 125.50, 113.36, 94.07, 45.98, 38.36, 37.34, 30.79, 21.57, 17.99, 14.06. HRMS (ESI) m/z Found 514.2709 $[M]^+$, calculated 514.2700 for $C_{31}H_{36}N_3O_4^+$.

2.1.2. Synthesis of CA532

Rho6G-MABA (20 mg, 0.04 mmol) and TSTU (14 mg, 0.05 mmol) were dissolved in 3 mL DMF under a nitrogen atmosphere. After added DIPEA (34 μL, 0.20 mmol), the reaction was stirred at room temperature for 30 min. Then a solution of mafenide hydrochloride (10 mg, 0.05 mmol) in DMF (1 mL) was added. The reaction was stirred an additional 12 h at room temperature. After the reaction is complete, the solvent was removed under reduced pressure. The crude product was purified by silica gel chromatography (MeOH /DCM = 5:1; V/V) to afforded **CA532** as a purple red solid 11 mg, yield 41 % . ^{1}H NMR (400 MHz, MeOD) δ 7.77 (d, J = 8.3 Hz, 2 H), 7.66 (dd, J = 5.4, 3.5 Hz, 2 H), 7.59 (d, J = 3.4 Hz, 1 H), 7.42 (dd, J = 5.8, 3.0 Hz, 1 H), 7.29 (d, J = 8.2 Hz, 2 H), 6.95 (s, 2 H), 6.76 (s, 2 H), 4.27 (s, 2 H), 3.40 (dt, J = 21.6, 7.3 Hz, 4 H), 3.11 (t, J = 7.2 Hz, 2 H), 2.85 (s, 3 H), 2.08 (s, 6 H), 1.69 (t, J = 7.5 Hz, 2 H), 1.35–1.17 (m, 8 H). ^{13}C NMR (100 MHz, MeOD) δ 173.47, 169.24, 157.43, 156.40, 155.10, 143.36, 142.48, 136.10, 131.00, 130.23, 129.70, 129.55, 129.38, 127.38, 127.26, 126.00, 125.27, 113.42, 93.54, 46.16, 42.08, 38.10, 36.58, 32.24, 22.06, 16.09, 12.64. HRMS (ESI) m/z Found 682.3088 $[M]^+$, calculated 682.3058 for $C_{38}H_{44}N_5O_5S^+$.

2.2. Spectral measurements

The probe stock solution (2 mmol) was produced in DMSO unless otherwise stated, and the absorption and fluorescence spectra were measured in a standard quartz cuvette. The measured solutions (5 μM) were prepared by diluting the probe stock solutions to the corresponding concentration. λ_{ex} = 505 nm.

Rho6G was used to determine the relative fluorescence quantum yields of the substances **Rho6G-MABA** and **CA532** (Rho6G's fluorescence quantum yield in PBS is 0.95). And the well-established literature equation is employed to calculate quantum yield [28].

2.3. Living cells imaging

According to our published work, the cytotoxicity of **CA532** was tested prior to cell imaging using the conventional MTT assay [29]. HeLa cells were cultured in a humidified atmosphere of 5 % CO_2/95 % air at 37 °C to reach 60–80 % confluency, then transfected CAIX plasmids by Lipofectamine 2000 (Invitrogen) according to the manufacturer's protocol. And for cell membrane imaging, cells were incubated with probe for 10 min at 37 °C, then directly used for cell membrane protein CAIX

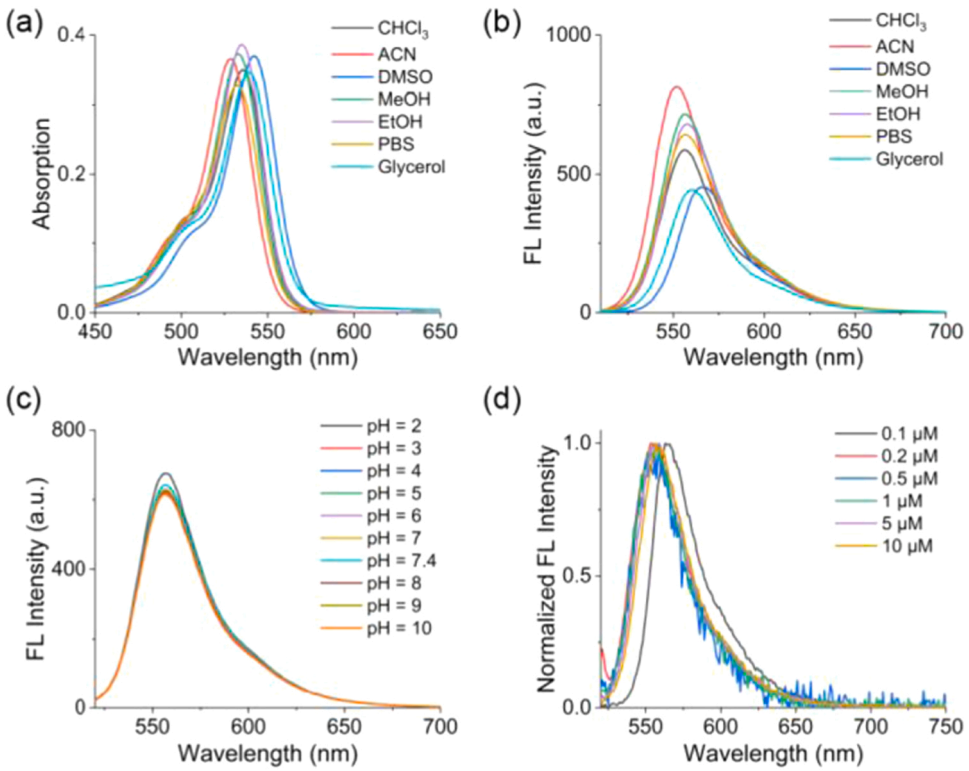

Fig. 2. (a) Absorption and (b) fluorescence spectra of 5 μM **Rho6G-MABA** in various solvents; (c) fluorescence spectra of 5 μM **Rho6G-MABA** in different pH buffer solutions; (d) normalized fluorescence intensity spectra of different concentrations of **Rho6G-MABA** in PBS (10 mM, pH = 7.4).

imaging.

For long-term confocal imaging, we incubate the CAIX -transfected HeLa cells with **CA532** for 10 min, and then directly used for cell membrane protein CAIX imaging and take one image every 10 min for a total of 2 h.

2.4. Fluorescent competition in living cells

For inhibitor inhibition rate assay, living HeLa cells which transfected CAIX protein were incubated with **CA532** for cell membrane imaging, then inhibitor was added to the cell dish without any wash and one image was collected every 5 s for a total of 5 min.

For inhibitor competition assay for membrane-bound CAIX protein on HeLa cells. The concentration of probe **CA532** was fixed at 500 nM in each experiment. Following the addition of the probe to the HeLa cells cultivated with transfected CAIX plasmids, a stock solution of each inhibitor was added to the cells stained with the probe, and fluorescence imaging was performed without any washing processes. After each concentration of inhibitor was added, incubated for 10 min, imaged, and averaged from three fields of view. All of the average intensity of cell membrane was calculated by using imageJ plug in MorphoLibJ [30].

3. Results and discussion

3.1. Design of CA532

In the indicator-displacement assay for cellular membrane proteins, the optical and chemical properties of the fluorescent inhibitor (fluorescent probe) are crucial. The ideal fluorescent probe should possess a high signal-to-noise ratio, excellent photostability, and a lengthy cell membrane retention period. As shown in Fig. 1, rhodamine 6G was selective as the fluorophore for its high brightness and photostability. The linking group 4-(methylamino)butanoic acid dramatically reduced the permeability of rhodamine dyes through cell membranes. With benzenesulfonamide serving as the targeting group for carbonic anhydrase, the lowered inhibitory activity can greatly expand the probe's detection range. Due to its binding with CAIX protein, the fluorescence is boosted when the probe aggregates to the cell membrane; when an inhibitor competes with the probe, the probe is re-released to the cell culture and the fluorescence on cellular membrane is quenched, enabling selective imaging of inhibitor activity.

3.2. Optical properties of CA532

Rhodamine dyes have high quantum yields and absorbance and are widely used for biological labeling and tracking [31–33]. However, for molecules such as tetramethylrhodamine or Rhodamine B, the two ends of the conjugated system use dialkylamino groups as electron-donating groups, respectively. During the excitation process of absorbing light, a twisted intramolecular charge transfer (TICT) will occur, resulting in fluorescence quenching [28]. In the Rhodamine 6G dye, the two ends of the conjugated system are used as electron-donating groups by ethylamino groups to reduce the possibility of generating TICT, which makes Rhodamine 6G have a very high quantum yield. As shown in Table S1 and Fig. 2, CA532 maintains a quantum yield close to 1 in aqueous solution. Compared with Rhodamine 6G and the precursor compound **Rho6G-MABA**, the molar extinction coefficient of **CA532** also did not change, the absorption and emission wavelengths in different solvents also changed little, and the emission wavelength was not affected by pH and dye concentrations. (Table S1) These results all indicate that **CA532** is uniformly dispersed in aqueous solution, and the fluorescence emission is not affected by the environment and remains stable. To our knowledge, **CA532** is one of the brightest sulfonamide wash-free substrates reported so far (Table S2: comparison with reported fluorescent substrates).

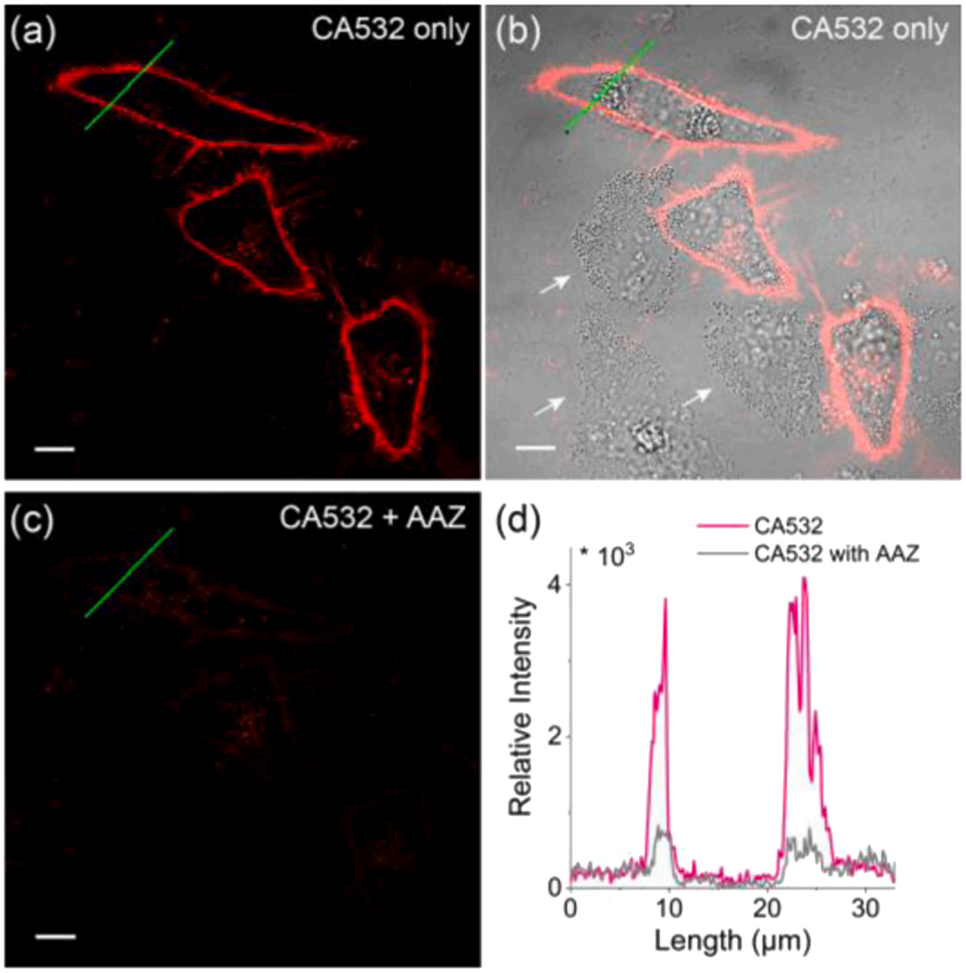

Fig. 3. Wash-free imaging of cell membrane protein CAIX in living cells using **CA532**. HeLa cells were transfected with CAIX plasmids. (a) Confocal imaging of HeLa cells stained with **CA532** (500 nM) and (b) merged with bright fields. White arrows indicated those HeLa cells with no plasmid transfected. (c) The addition of inhibitor AAZ (10 μM) to the cell dish, incubated with 1 min (d) Intensity profile of regions of interest (ROI) across green line. Scale bar: 10 μm.

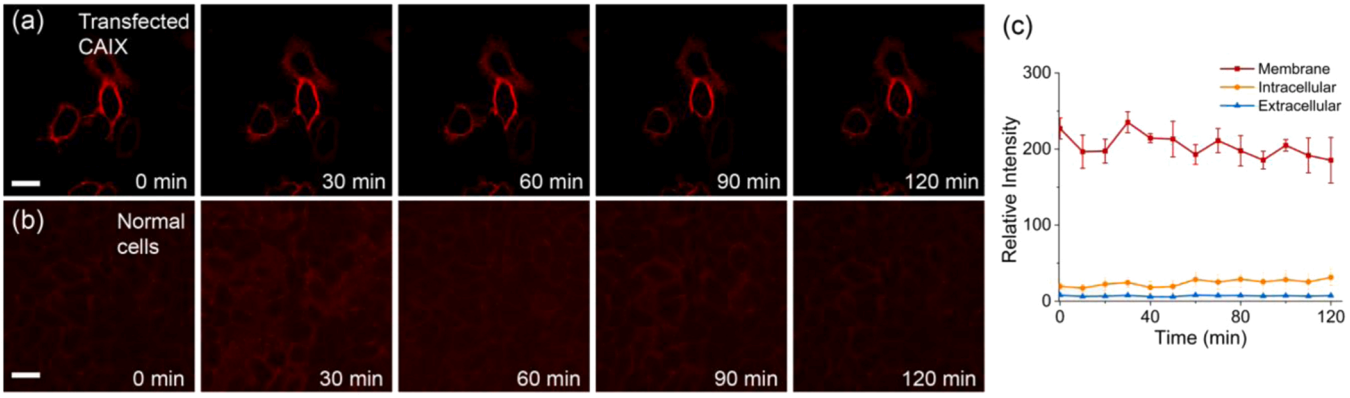

Fig. 4. Cell impermeable capacity of probe **CA532**. (a) Long-term confocal imaging of HeLa cells transfected with membrane protein CAIX, and cells were stained with **CA532** (500 nM). (b) Long-term confocal imaging of normal HeLa cells stained with **CA532** (500 nM). (c) The relative fluorescence intensity changes of cell membrane, intracellular space, and extracellular space within two hours in (a). Scale bar: 20 μm.

3.3. Wash-free and long-term imaging of CAIX

MTT assays were used to examine the toxicity of **CA532** to HeLa cells before it was used in biological imaging (Fig. S1). After incubating normal HeLa cells with varying concentrations of **CA532** for 24 h, the cell viability always maintains a high survival rate (90 %), showing that the **CA532** has low cytotoxicity. Following that, fluorescence imaging in vitro was done to assess its detection ability in HeLa cells transfected CAIX plasmids. As shown in Fig. 3, **CA532** could specifically label the plasma membrane and exhibited excellent signal-to-noise ratios of 15 folds. In contrast, untransfected HeLa cells indicated by white arrows have no fluorescent signal from the cell membrane. After 1 min of incubation with the inhibitor acetazolamide (AAZ), the fluorescence signal on the cell membrane immediately reduced to one-seventh of its

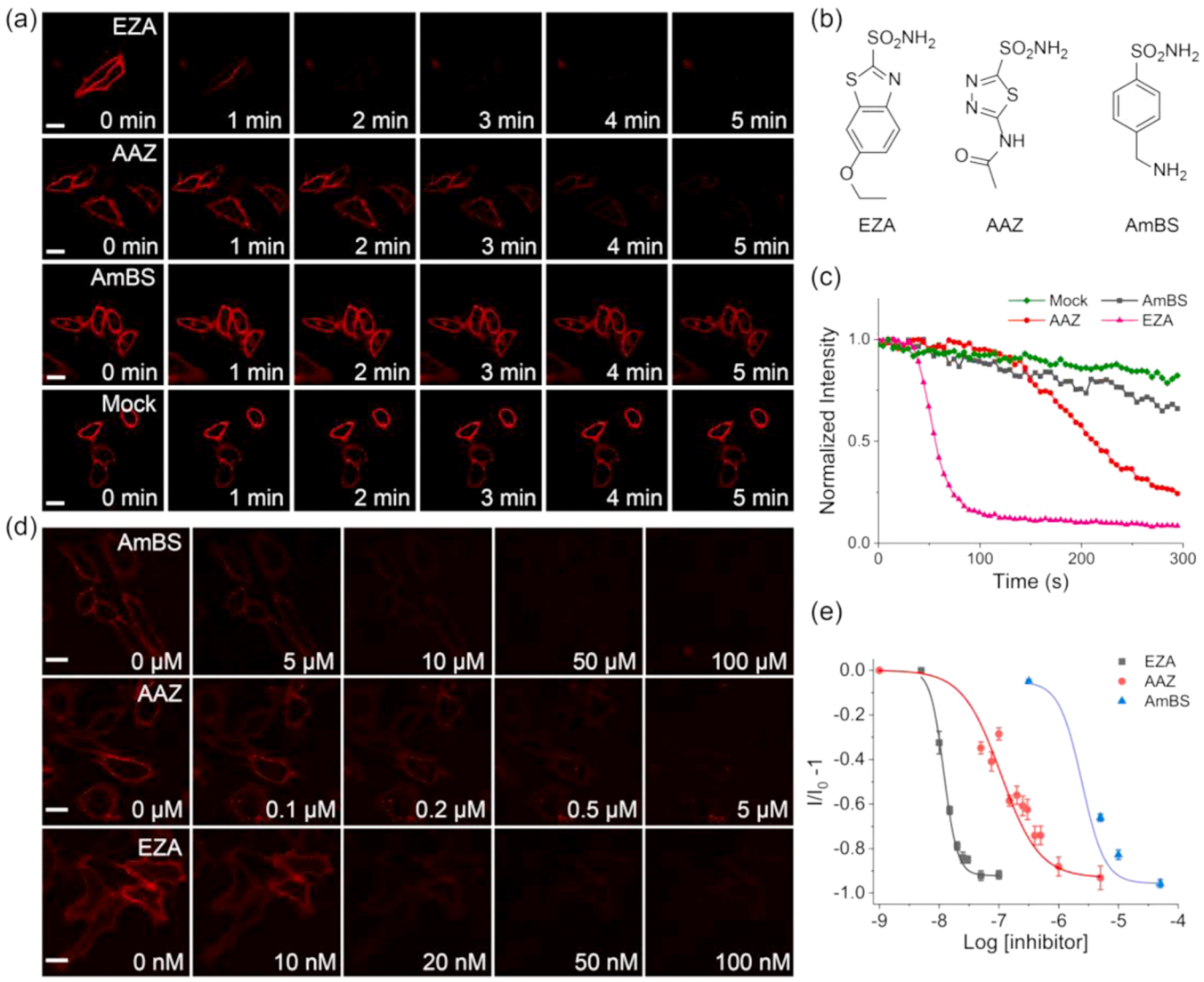

Fig. 5. Evaluation of membrane protein (CAIX) inhibitors activity and screening. (a) Confocal fluorescence imaging of different inhibitors incubated with living HeLa cells (preincubated with 500 nM **CA532**) which transfected with CAIX plasmids: first line with 5 μM EZA, second line with 5 μM AAZ, third line with 5 μM AmBS, and fourth line without any drugs. (b) Chemical structures of different inhibitors for CAIX protein. (c) Time-dependent changes of fluorescence intensity on cell membrane obtained from (a). (d) Fluorescence imaging of HeLa cells transfected with CAIX protein treated with probe **CA532** (500 nM) in the absence or presence of inhibitors. (e) Fluorescence titration assays of the relative fluorescence intensity changes on cell membrane ($I/I_0 - 1$) as functions of inhibitors' concentration. Inhibitor concentration: mol. Scale bar: 20 μm.

initial level.

We further tested the membrane permeability of the probe. The probe **CA532** can produce stable imaging for up to two hours in HeLa cells transfected with CAIX protein, and the fluorescence intensity is still stable at more than 90 % after two hours (Fig. 4). Simultaneously, we imaged normal HeLa cells and a weak fluorescence signal was observed on the cell membrane, which could be attributed to the probe's lipid solubility, which causes it to have an affinity for cell membrane lipids. These results indicate that the probe **CA532** is impermeable to the membrane, and evenly dispersed outside the cell membrane, because the concentration is very low, the background fluorescence intensity is very small, and it is difficult to affect the cell membrane imaging. When bound to target proteins in the cell membrane, the dye emits high-brightness fluorescence due to the marked increase in the local concentration of the dye, enabling wash-free cell membrane imaging. The excellent photostability of rhodamine 6 G also provides a basis for subsequent fluorescence imaging to track the dynamic process of binding and dissociation of small molecule protein complexes. It is worth noting that the fluorescent staining of cell membrane proteins has always had the problem that fluorescent substrates are easy to penetrate the membrane. The membrane-impermeable and uniformly dispersed fluorescent ligands such as Rho6G-MABA provide the possibility to derive fluorescent substrates targeting other membrane proteins. In the follow-up work, we will conjugate other functional small molecule groups in Rho6G-MABA through the generation of amides, and carry out more work on the imaging of cell membrane functional proteins and the screening of inhibitors.

3.4. Dynamic binding-dissociation images of CA532 for inhibitor screening

We comprehensively assessed the potential utility of this model in membrane protein inhibitor screening which using the reversible binding-dissociation dynamic imaging of fluorescent inhibitor **CA532** with CAIX protein. Therefore, we first tried to evaluate the inhibition rate of membrane proteins by three commercial carbonic anhydrase inhibitors (AmBS, AAZ and EZA) (Fig. 5). After staining with **CA532** (0.5 μM), the HeLa cells which transfected CAIX plasmids were mixed

with several CA inhibitors, and changes in fluorescence were imaged without any washing operations. When the stronger inhibitor EZA (5 μM) was added to the culture medium, a significant decrease in fluorescent intensity at the cell surface was induced, and the time for the intensity drop to half was only 42 s. As for moderate inhibitor AAZ (5 μM), the fluorescence intensity reduced more slowly, and takes 212 s to halve. In contrast, with weaker inhibitors AmBS (5 μM) or no inhibitors (only DMSO), only small changes in fluorescence were observed (Fig. 5a-c). Finally, dynamic binding-dissociation imaging-based drug screening for CAIX was performed on live HeLa cells which transfected CAIX plasmids using probe **CA532**. Based on the titration curves, the IC_{50} values of these three carbonic anhydrase inhibitors were calculated to be 12 nM for EZA, 105 nM for AAZ and 2.5 μM for AmBS. However, the literature values (K_i) for CAIX protein were reported to be 34 nM (EZA), 25 nM (AAZ), and 103 nM (AmBS), respectively [34]. It is obvious that the inhibitory activities of AAZ and AmBS obtained by us are quite different from those reported in the literature. Since the data in the literature were obtained from purified proteins and ours was obtained from cell imaging, these differences may be due to differences in the test system. Considering the fact that protein activity can only be maintained in situ on living cells, we believe that in situ detection of cell membrane protein inhibitors is crucial in order to completely assess the inhibitors' efficacy. As a result, cell membrane affinity may affect inhibitor binding and may reduce the inhibitory capabilities of AAZ and AmBS.

4. Conclusions

In summary, we have developed a probe **CA532** for wash-free imaging membrane protein CAIX and a screening test for membrane protein inhibitors in situ was conceived. Generally, probes used to detect the activity of cell membrane protein inhibitors like **CA532** must have the following properties: 1) high fluorescence brightness, stability and signal-to noise ratio, which reduces non-specific fluorescence fluctuations in detection; 2) appropriate target affinity and low cytotoxicity; 3) cell membrane impermeability to reduce the effect of intracellular fluorescent signal on detection. Because it removes the necessity for employ separate pure proteins for candidate small molecule drugs screening, the idea of cell membrane fluorescence inhibitor competition assays for inhibitor detection is generalizable and has extensive applicability. And then, many small molecule inhibitors based on cell membrane proteins, including CAIX protein, have been developed and reported; these inhibitors could use our assay to utilized to rapidly examine the inhibitory activity in situ. We believe that our probe and fluorescent competition assay facilitates for broad investigation into membrane protein inhibitors.

CRediT authorship contribution statement

W.Z., Y.T., W.J. and X.F. synthesized the probe and examined optical properties. W.Z., J.L. and N.X. did the cell imaging. W.Z., Q.Q. and Z.X. wrote the paper.

Declaration of Competing Interest

The authors declare that they have no known competing financial interests or personal relationships that could have appeared to influence the work reported in this paper.

Data Availability

I have shared the data as in Supporting Information file.

Acknowledgements

We are grateful for the financial support from the National Natural Science Foundation of China (22225806, 22078314, 21878286, 22278394, 21908216), Dalian Institute of Chemical Physics (DICP I202142, DICP I202227) and Dalian Science and Technology Innovation Plan (2022JJ11CG007).

Appendix A. Supporting information

Supplementary data associated with this article can be found in the online version at doi:10.1016/j.snb.2022.132980.

References

[1] Z. Cournia, T.W. Allen, I. Andricioaei, B. Antonny, D. Baum, G. Brannigan, et al., Membrane protein structure, function, and dynamics: a perspective from experiments and theory, J. Membr. Biol. 248 (2015) 611–640.
[2] G. Várady, J. Cserepes, A. Németh, E. Szabó, B. Sarkadi, Cell surface membrane proteins as personalized biomarkers: where we stand and where we are headed, Biomark. Med 7 (2013) 803–819.
[3] Y. Chen, C. Xue, J. Wang, M. Xu, Y. Li, Y. Ding, et al., High-contrast and real-time visualization of membrane proteins in live cells with malachite green-based fluorogenic probes, Chin. Chem. Lett. 33 (2022) 1637–1642.
[4] R. Santos, O. Ursu, A. Gaulton, A.P. Bento, R.S. Donadi, C.G. Bologa, et al., A comprehensive map of molecular drug targets, Nat. Rev. Drug Disco 16 (2017) 19–34.
[5] M. Stocks, Chapter 3 - The small molecule drug discovery process – from target selection to candidate selection, in: R. Ganellin, S. Roberts, R. Jefferis (Eds.), Introduction to Biological and Small Molecule Drug Research and Development, Elsevier, Oxford, 2013, pp. 81–126.
[6] K. Mizusawa, Y. Takaoka, I. Hamachi, Specific cell surface protein imaging by extended self-assembling fluorescent turn-on nanoprobes, J. Am. Chem. Soc. 134 (2012) 13386–13395.
[7] X. Xu, Z. Kuang, J. Han, Y. Meng, L. Li, H. Luan, et al., Development and characterization of a fluorescent probe for gls1 and the application for high-throughput screening of allosteric inhibitors, J. Med. Chem. 62 (2019) 9642–9657.
[8] C. Prével, M. Pellerano, T.N.N. Van, M.C. Morris, Fluorescent biosensors for high throughput screening of protein kinase inhibitors, Biotechnol. J. 9 (2014) 253–265.
[9] K.E. Prosser, A.J. Kohlbrand, H. Seo, M. Kalaj, S.M. Cohen, 19F-Tagged metal binding pharmacophores for NMR screening of metalloenzymes, Chem. Commun. 57 (2021) 4934–4937.
[10] D.A. Annis, E. Nickbarg, X. Yang, M.R. Ziebell, C.E. Whitehurst, Affinity selection-mass spectrometry screening techniques for small molecule drug discovery, Curr. Opin. Chem. Biol. 11 (2007) 518–526.
[11] W. Li, B. Zhang, Z. Chen, Screening carbonic anhydrase IX inhibitors in traditional Chinese medicine based on electrophoretically mediated microanalysis, Talanta 232 (2021), 122444.
[12] H.O. Tawfik, A. Petreni, C.T. Supuran, M.H. El-Hamamsy, Discovery of new carbonic anhydrase IX inhibitors as anticancer agents by toning the hydrophobic and hydrophilic rims of the active site to encounter the dual-tail approach, Eur. J. Med Chem. 232 (2022), 114190.
[13] H. Yin, A.D. Flynn, Drugging membrane protein interactions, Annu. Rev. Biomed. Eng. 18 (2016) 51–76.
[14] E. Andrea, Rawlings, Membrane proteins: always an insoluble problem? Biochem. Soc. Trans. 44 (2016) 790–795.
[15] T.H. Maren, Carbonic anhydrase: chemistry, physiology, and inhibition, Physiol. Rev. 47 (1967) 595–781.
[16] C.T. Supuran, Carbonic anhydrases: novel therapeutic applications for inhibitors and activators, Nat. Rev. Drug Disco 7 (2008) 168–181.
[17] A. Kumar, K. Siwach, C.T. Supuran, P.K. Sharma, A decade of tail-approach based design of selective as well as potent tumor associated carbonic anhydrase inhibitors, Bioorg. Chem. 126 (2022), 105920.
[18] J. Li, G. Zhang, X. Wang, X.-F. Li, Is carbonic anhydrase IX a validated target for molecular imaging of cancer and hypoxia? Future Oncol. 11 (2015) 1531–1541.
[19] A.C. Sedgwick, J.T. Brewster, T. Wu, X. Feng, S.D. Bull, X. Qian, et al., Indicator displacement assays (IDAs): the past, present and future, Chem. Soc. Rev. 50 (2021) 9–38.
[20] Z. Xiao, D. Chen, S. Song, R. van der Vlag, P.E. van der Wouden, R. van Merkerk, et al., 7-Hydroxycoumarins are affinity-based fluorescent probes for competitive binding studies of macrophage migration inhibitory factor, J. Med. Chem. 63 (2020) 11920–11933.
[21] J.C. Chang, I.D. Tomlinson, M.R. Warnement, H. Iwamoto, L.J. DeFelice, R. D. Blakely, et al., A fluorescence displacement assay for antidepressant drug discovery based on ligand-conjugated quantum dots, J. Am. Chem. Soc. 133 (2011) 17528–17531.
[22] H. Zhang, P. Xu, X. Zhang, X. Cao, W. Han, M. Liu, et al., Au nanoparticles based ultra-fast "Turn-On" fluorescent sensor for detection of biothiols and its application in living cell imaging, Chin. Chem. Lett. 31 (2020) 1083–1086.
[23] S. Jiang, W. Mao, D. Mao, Z.-T. Li, D. Ma, AND molecular logic gates based on host-guest complexation operational in live cells, Chin. Chem. Lett. 33 (2022) 881–884.
[24] Y. Jiao, S. Lan, D. Ma, Ultra-stable and multistimuli-responsive nanoparticles coated with zwitterionic pillar[n]arene for enhanced cellular uptake, Chin. Chem. Lett. 32 (2021) 1025–1028.

[25] P.E.Z. Klier, J.G. Martin, E.W. Miller, Imaging reversible mitochondrial membrane potential dynamics with a masked rhodamine voltage reporter, J. Am. Chem. Soc. 143 (2021) 4095–4099.
[26] N. Wang, Y. Hao, X. Feng, H. Zhu, D. Zhang, T. Wang, et al., Silicon-substituted rhodamines for stimulated emission depletion fluorescence nanoscopy, Chin. Chem. Lett. 33 (2022) 133–140.
[27] F. Deng, Z. Xu, Heteroatom-substituted rhodamine dyes: structure and spectroscopic properties, Chin. Chem. Lett. 30 (2019) 1667–1681.
[28] W. Zhou, X. Fang, Q. Qiao, W. Jiang, Y. Zhang, Z. Xu, Quantitative assessment of rhodamine spectra, Chin. Chem. Lett. 32 (2021) 943–946.
[29] J. Chen, C. Wang, W. Liu, Q. Qiao, H. Qi, W. Zhou, et al., Stable super-resolution imaging of lipid droplet dynamics through a buffer strategy with a hydrogen-bond sensitive fluorogenic probe, Angew. Chem. Int. Ed. 60 (2021) 25104–25113.
[30] D. Legland, I. Arganda-Carreras, P. Andrey, MorphoLibJ: integrated library and plugins for mathematical morphology with ImageJ, Bioinformatics 32 (2016) 3532–3534.
[31] F. Deng, D. Sun, S. Yang, W. Huang, C. Huang, Z. Xu, et al., Comparison of rhodamine 6G, rhodamine B and rhodamine 101 spirolactam based fluorescent probes: a case of pH detection, Spectrochim. Acta Part A: Mol. Biomol. Spectrosc. 268 (2022), 120662.
[32] W. Liu, J. Chen, Q. Qiao, X. Liu, Z. Xu, A TICS-fluorophore based probe for dual-color GSH imaging, Chin. Chem. Lett. 33 (2022) 4943–4947.
[33] Q. Qiao, W. Liu, J. Chen, X. Wu, F. Deng, X. Fang, et al., An acid-regulated self-blinking fluorescent probe for resolving whole-cell lysosomes with long-term nanoscopy, Angew. Chem. Int. Ed. 61 (2022), e202202961.
[34] V. Garaj, L. Puccetti, G. Fasolis, J.-Y. Winum, J.-L. Montero, A. Scozzafava, et al., Carbonic anhydrase inhibitors: synthesis and inhibition of cytosolic/tumor-associated carbonic anhydrase isozymes I, II, and IX with sulfonamides incorporating 1,2,4-triazine moieties, Bioorg. Med Chem. Lett. 14 (2004) 5427–5433.

Wei Zhou obtained his B.S. degree from school of Chemical and Material Engineering, Jiangnan University in 2019. He is currently working toward the Ph.D. degree in organic chemistry with the Dalian University of Technology. His research interest is the structure-fluorescence relationship of rhodamine dyes.

Qinglong Qiao obtained his Ph.D. from Dalian University of Technology in 2018. He is currently an associate professor at the Dalian Institute of Chemical Physics, Chinese Academy of Sciences. His research interest is the development of new fluorophore, fluorescent probe designing and super-resolution fluorescence imaging.

Yi Tao obtained her B.S. degree from Zhang Dayu School of Chemistry, Dalian University of Technology in 2020. She is currently working toward the Ph.D. degree in analytical chemistry with the Dalian Institute of Chemical Physics. Her research interest is the structure-fluorescence relationship of rhodamine dyes.

Wenchao Jiang obtained his B.S. degree from Wuhan University of Technology in 2018. He is currently working toward the Ph.D. degree in Dalian Institute of Chemical Physics. His research interest is the TICT mechanism.

Xiangning Fang obtained her B.S. degree from East China University of Science and Technology in 2019. She is currently working toward the Ph.D. degree in Dalian Institute of Chemical Physics.

Jin Li obtained her M.S. degree from Lanzhou Institute of Chemical Physics in 2017. She is currently working toward the Ph.D. degree in Dalian Institute of Chemical Physics.

Ning Xu obtained his M.S. degree from Shandong University of technology in 2018. He is currently working toward the Ph.D. degree in Dalian University of Technology. His research interest is the TICT mechanism.

Zhaochao Xu was born in Qingdao, China, in 1979. He received his Ph.D. in 2006 from Dalian University of Technology under the supervision of Prof. Xuhong Qian. Subsequently, he joined Prof. Juyoung Yoon's group at Ewha Womans University as a post-doctoral researcher. Since October 2008, he was a Herchel Smith Research Fellow at University of Cambridge in Prof. David R. Spring's group. In 2011, he moved to Dalian Institute of Chemical Physics, CAS, where he is currently a Professor. His research is focusing on new fluorophore design and structure-fluorescence relationship, protein labelling and sensing, the development of fluorescent probes for the selective recognition and fluorescent imaging of biologically important species, and super-resolution fluorescent imaging.